

**WATER-MODERATED HEXAGONALLY PITCHED LATTICES OF
U(90%)O₂ + CU FUEL RODS WITH GD OR SM RODS**

Evaluators

**Andrey Yu. Gagarinski
Vladimir D. Pavlov
Russian Research Center "Kurchatov Institute"**

**Internal Reviewer
Andrey A. Bykov**

Independent Reviewer

**Virginia F. Dean
Consultant to Idaho National Engineering Laboratory**

WATER-MODERATED HEXAGONALLY PITCHED LATTICES OF U(90%)O₂ + CU FUEL RODS WITH GD OR SM RODS

IDENTIFICATION NUMBER: HEU-COMP-THERM-004

KEY WORDS: acceptable, absorber, critical experiment, cross-shaped, gadolinium, highly enriched, lattices, samarium, spiral, ²³⁵U, water-moderated

1.0 DETAILED DESCRIPTION

1.1 Overview of Experiment

A series of critical experiments with water-moderated hexagonally pitched lattices with highly enriched (approximately 90% ²³⁵U) fuel rods of cross-shaped cross section was performed in 1969 at RRC "Kurchatov Institute" (see References 1 and 2). These experiments consisted of double lattices of fuel rods and absorber rods containing Gd or Sm. Double lattices are two superimposed lattices of two different types of rods at different pitches. Rods of the larger-pitched lattice replace those of the other lattice.

This evaluation describes 4 critical configurations of hexagonal lattices of fuel rods and Gd or Sm rods. The fuel rod lattice pitch value was 5.3 mm for all experiments. The absorber rod lattice pitch values were approximately 27.5 and 36.7 mm. All four configurations are considered to be acceptable for use as benchmark critical experiments.

1.2 Description of Experimental Configuration

Experiment Tank and Surroundings. Experiments were performed in a 15-mm-thick, open-top, stainless-steel tank (see Figure 1). The tank inside diameter was 1600 mm and its height was 2000 mm. The top level of the tank coincided with a concrete floor of the experiment room. The tank support ring sat upon the concrete floor. The critical assembly upper support ring lay upon the tank support ring. All details of the assembly, including bottom support plate, fuel rods support plate, and lattice plates, were fixed to the upper support ring by six 40-mm-diameter stainless steel rods. The distance between these rods and the core was more than 450 mm, so they had no influence on critical conditions. A stand was placed between the fuel rod support plates and bottom AD1 aluminum alloy support plate. The stand was a hollow hexagonal prism with 6 plates within, made of 5-mm-thick AD1 aluminum alloy plates (see Figures 1 and 2).

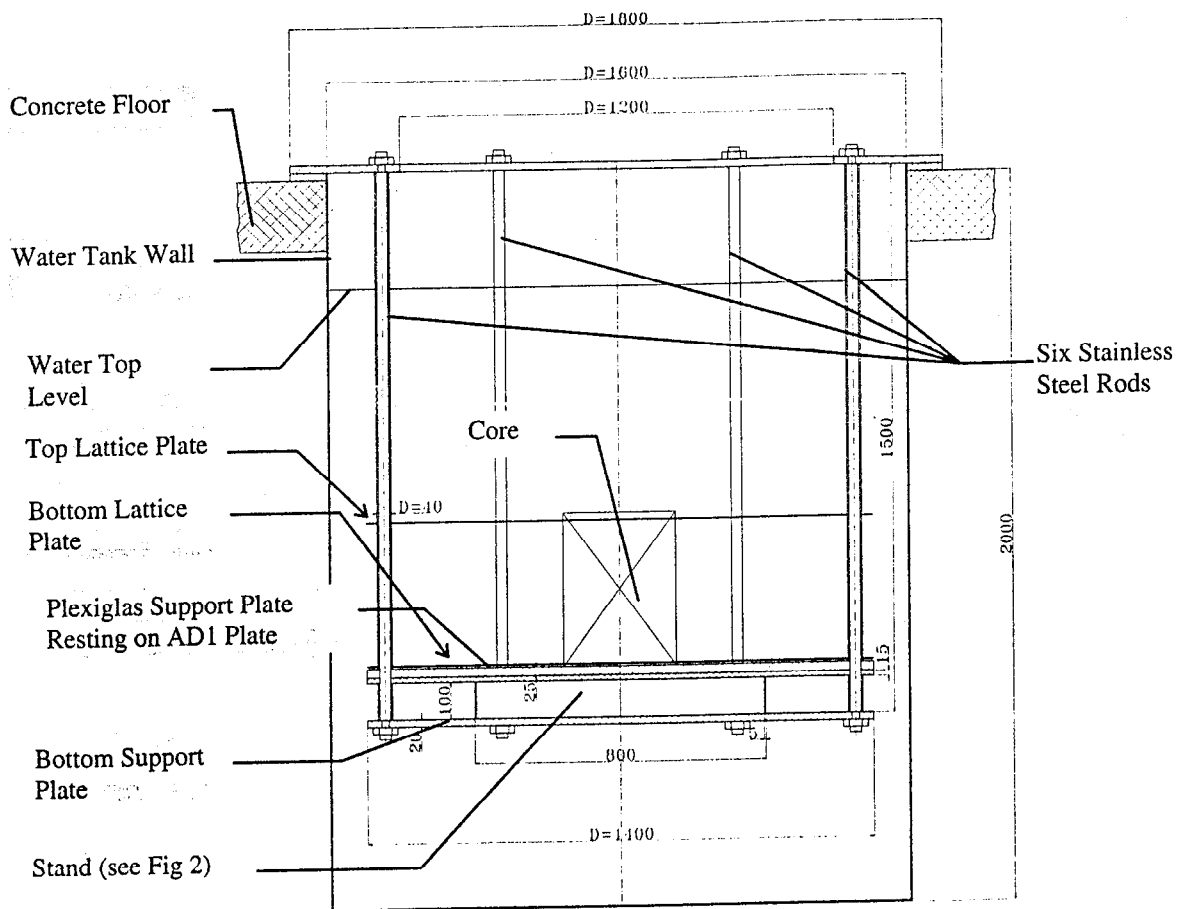


Figure 1. Configuration of the Critical Assembly with Water Tank. (dimensions given in mm)

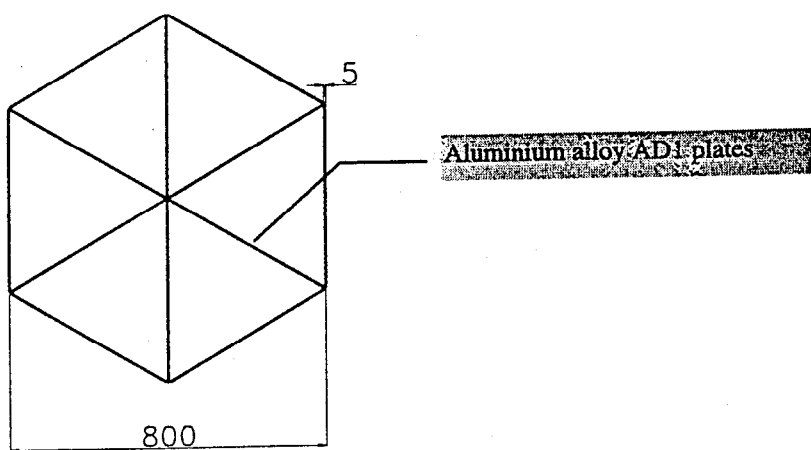


Figure 2. Cross Section of the Stand (see Figure 1). (dimensions given in mm)

Fuel Rod Support Plates. The bottoms of the fuel rods were supported by a 25-mm-thick Plexiglas plate resting on a 15-mm-thick AD1 aluminum alloy support plate (see Figure 3).

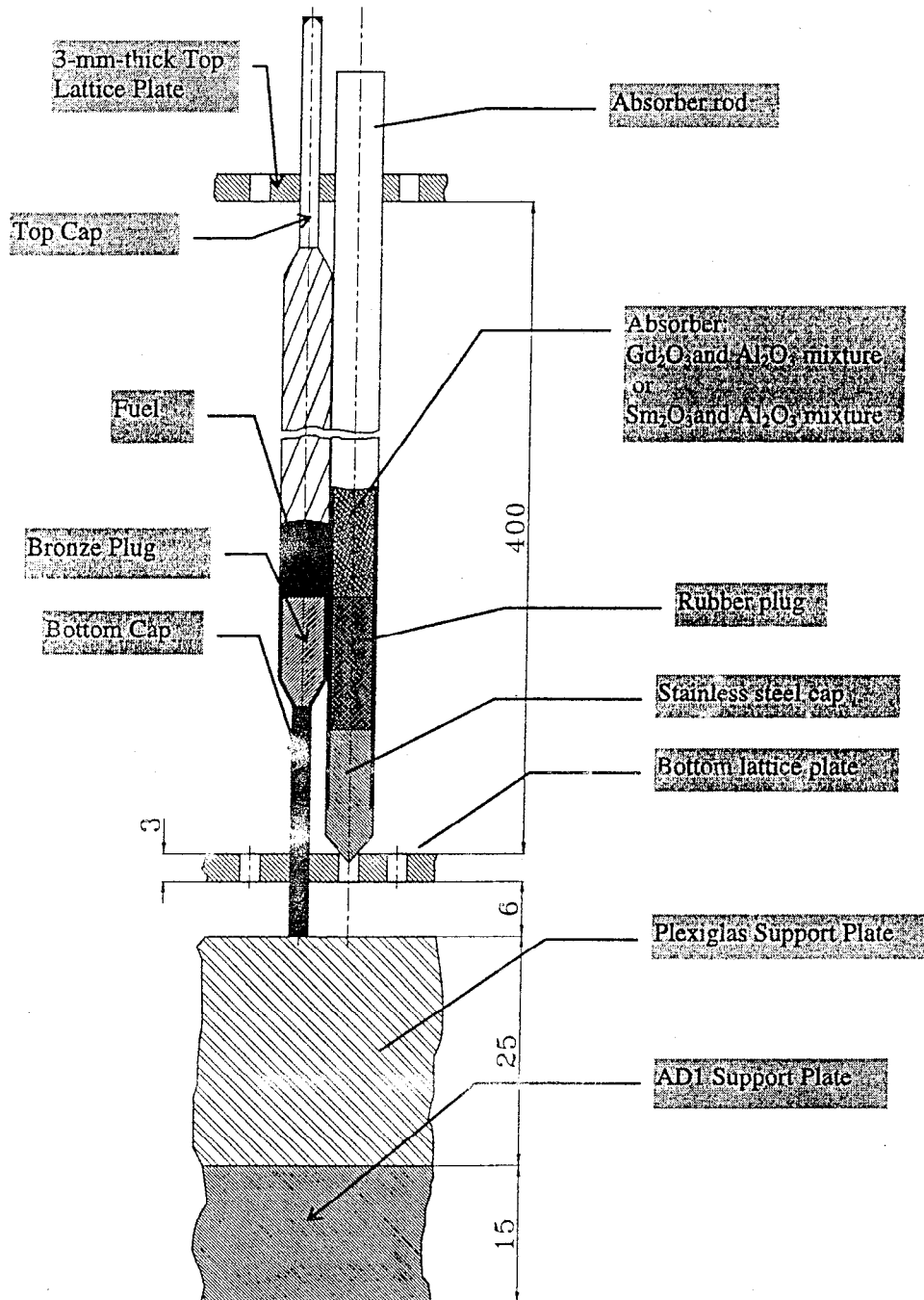


Figure 3. Schematic of the Fuel and Absorber Rods Placement in the Core.
(dimensions given in mm)

Lattice Plates. The pitch of the fuel rods was maintained by two 3-mm-thick AD1 aluminium alloy lattice plates. Holes for the fuel rod caps were no more than 0.2 mm larger than the fuel rod cap diameter, as were holes for the absorber rods in the top lattice plate, which also were no more than 0.2 mm larger than the absorber rod diameter. Figure 3 shows a schematic of the fuel and absorber rods' placement in the core.

Water Reflector. The top water surface was at least 200 mm above the top of the fuel region. The bottom water reflector was at least 500 mm thick. The radial reflector was greater than 500 mm thick. Therefore all reflectors were effectively infinite.

Control and Safety Rods. There were six 8-mm-diameter boron carbide control and safety rods. The distance between the control rods and core was ~ 10 mm. The control rods were withdrawn at least 200 mm above the top of the fuel region for the reported configurations. The rods moved inside perforated aluminium tubes (12 mm outer diameter, 8 mm inner diameter) in the radial reflector. Eight steel tubes containing neutron detectors were located in the radial reflector. The distance between the neutron detectors and the fuel rods was ~200 mm. Measurements of the effects of removal of the tubes containing neutron detectors indicated that they had no influence on critical conditions.

Fuel Rods. Fuel rods had a "cross-shaped" cross section (see Figures 4 and 5). According to the fuel rods certificate, the fuel height was 344 ± 10 mm. According to measurements of approximately 30% of the rods, the average fuel height was 341 ± 4 mm. The fuel rod cross section was twisted with a 400-mm period to form a spiral shape. Fuel was replaced with bronze at both ends of the fuel region. The bronze plugs had the same "cross-shaped" cross section as the fuel region. The bottom bronze plug was 12 mm long, including the 3-mm-long tapered end. The height of the top bronze plug, which was varied together with the fuel region height, was approximately 12 mm. The fuel rod caps and clad were made of stainless steel. The caps had a diameter of 2 mm. The top and bottom cap height was 25 mm.

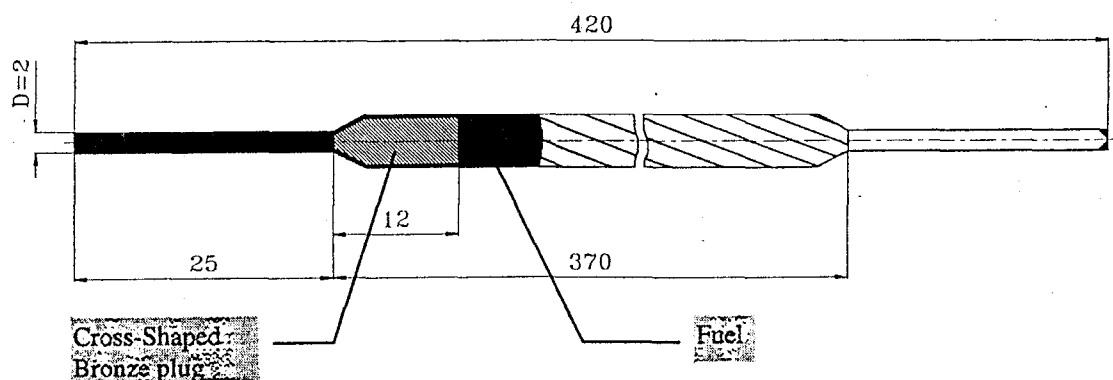


Figure 4. Spiral Cross-Shaped Fuel Rod. (dimensions given in mm)

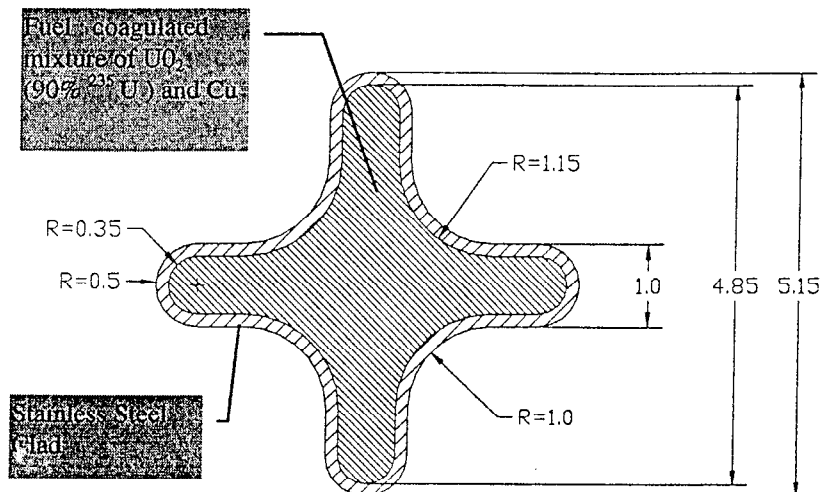


Figure 5. Cross-Section of Cross-Shaped Fuel Rod. (dimensions given in mm)

Absorber Rods. The absorber rods (see Figure 6) were made of 0.3-mm-thick stainless steel tubes. Their outer diameter was 5.10 ± 0.05 mm. Each rod was loaded with either a mixture of Gd_2O_3 and Al_2O_3 (gadolinium absorber rod) or a mixture of Sm_2O_3 and Al_2O_3 (samarium absorber rod). Each absorber rod had a stainless steel bottom cap and top and bottom rubber plugs (see Figure 6). The absorber rods were prepared especially for this series of experiments by the experimenters. The portions of Gd_2O_3 and Sm_2O_3 had been carefully weighed to an accuracy of better than 2% before being mixed with the Al_2O_3 .

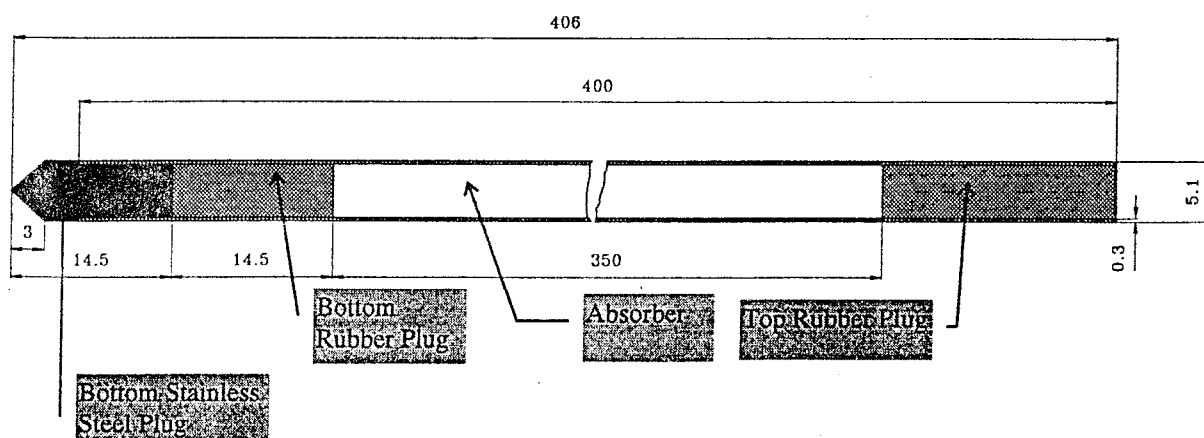


Figure 6. Absorber Rod. (dimensions given in mm)

1.2.1 Critical Configurations of the Hexagonal Lattices with Fuel Rods and Absorber Rods -

Two critical configurations of hexagonally pitched lattices with fuel rods and gadolinium absorber rods and two critical configurations of hexagonally pitched lattices with fuel rods and samarium absorber rods were assembled. The fuel rod lattice pitch values were 5.3 ± 0.02 mm for all experiments. The absorber rod lattice pitch values were 27.54 and 36.72 mm. A fuel-rods critical number was selected so that $k_{\text{eff}} = 1$ when the top water reflector height was at least 200 mm. The k_{eff} uncertainty in critical number of rods was determined by the reactivity changes for loading or unloading a single fuel rod and it was estimated as $\sim (\pm 0.5 \cdot 1) \cdot 10^{-4}$. The inherent experimental uncertainties in the determination of the critical number of fuel rods consisted of the uncertainty in the k_{eff} measurement and unknown factors whose effects were revealed by repeated measurements. These uncertainties did not include effects of geometrical and material compositions uncertainties.

To evaluate the reproduction uncertainties in k_{eff} , repeated experiments that included both a complete reloading of these cores and a simple water draining followed by water flooding were performed. The reproduction uncertainty in k_{eff} was estimated as $\sim 3 - 4 \cdot 10^{-4}$.

A measured estimate of the uncertainty in k_{eff} due to the effect of the control rod tubes was $\sim \pm 1 \cdot 10^{-4}$. Based on measurements of temperature effects, the same uncertainty is assigned to k_{eff} due to the effect of small deviations of the water temperature. The temperature of the critical assemblies varied in the range from 18°C to 20°C.

Therefore, the combined uncertainties in k_{eff} , except for those due to the effect of geometrical and material composition uncertainties, is $\sim 3 - 4 \cdot 10^{-4}$.

The fuel and absorber rod numbers for the four critical configurations are summarized in Table 1. Figures 7, 8, 9, and 10 give views of the critical configurations with absorber rod lattice pitch values of 27.54 and 36.72 mm for Gd and Sm absorbers.

Table 1. Fuel and Absorber Rod Numbers and Pitch Values
for Four Critical Configurations.

Case Number	Absorber	Absorber Rods Lattice Pitch Value (mm)	Critical Number of Fuel Rods	Number of Absorber Rods
1	Gd	27.54	2760	106
2	Gd	36.72	2520	55
3	Sm	27.54	3198	121
4	Sm	36.72	2727	58

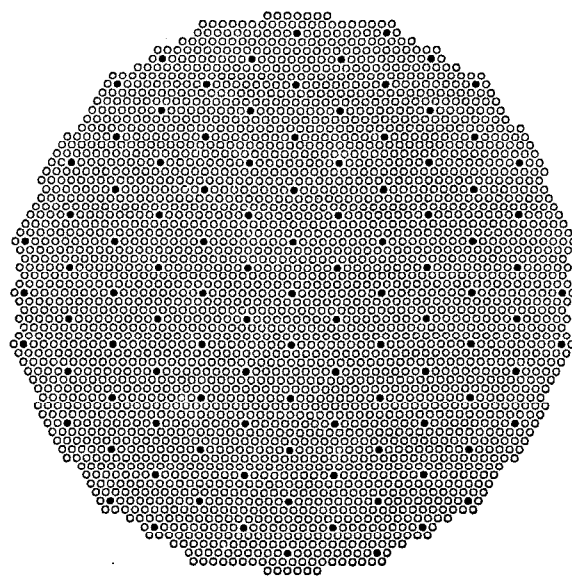


Figure 7. Critical Configuration of Case 1 Lattice with Fuel and Gd Absorber Rods.
(Fuel rod pitch is 5.3 mm, absorber rod pitch is ~27.5 mm.)

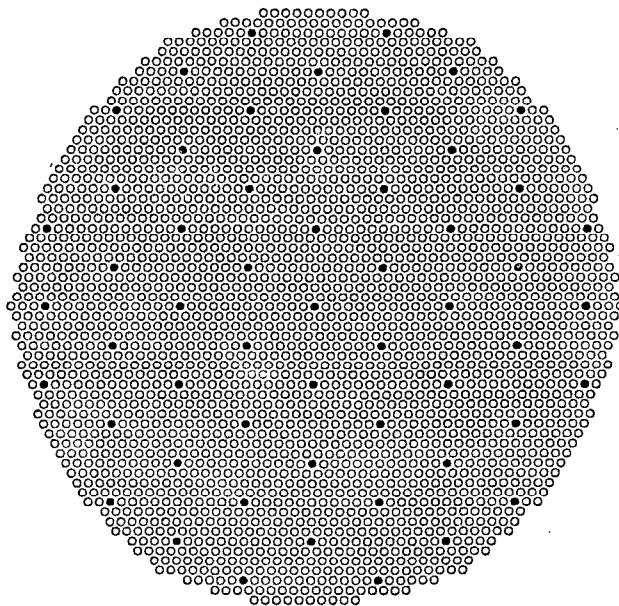


Figure 8. Critical Configuration of Case 2 Lattice with Fuel and Gd Absorber Rods.
(Fuel rod pitch is 5.3 mm, absorber rod pitch is ~36.7 mm.)

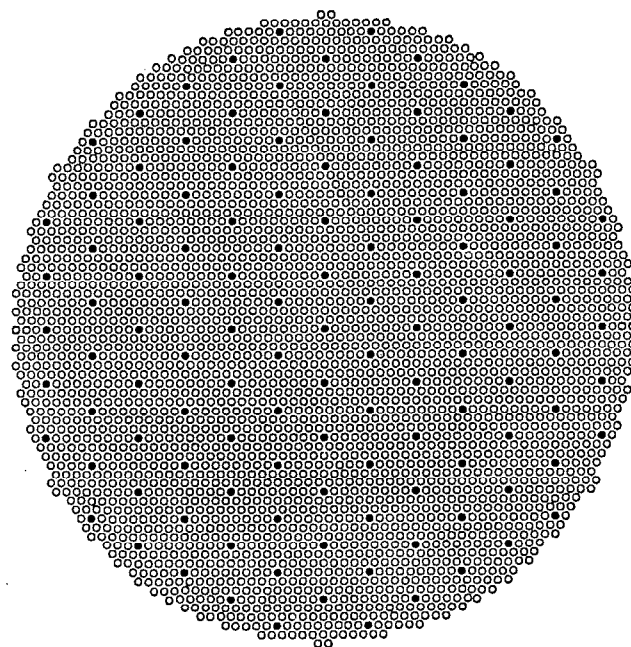


Figure 9. Critical Configuration of Case 3 Lattice with Fuel and Sm Absorber Rods.
(Fuel rod pitch is 5.3 mm, absorber rod pitch is ~27.5 mm.)

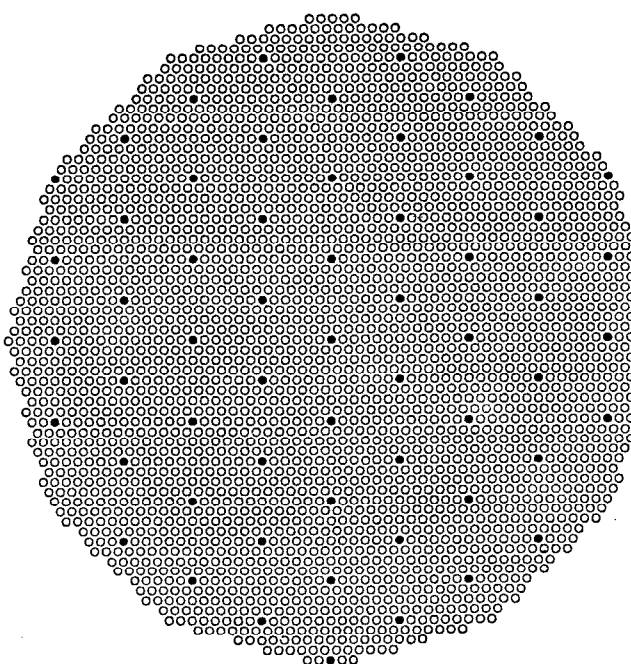


Figure 10. Critical Configuration of Case 4 Lattice with Fuel and Sm Absorber Rods.
(Fuel rod pitch is 5.3 mm, absorber rod pitch is ~36.7 mm.)

1.3 Description of Material Data

1.3.1 Fuel Rod Material Data - A coagulated mixture of UO₂, enriched in ²³⁵U to ~90 %, and Cu powder is used as the fission material of the fuel rods. Table 2 shows the isotopic composition of the fission material.

Table 2. Isotopic Composition of the Uranium.^(a)

Isotope	²³⁴ U	²³⁵ U	²³⁶ U	²³⁸ U
At.%	0.85±0.01	88.87±0.36	0.28±0.01	10.00±0.04

(a) Reference 2

Table 3 shows the average masses of materials in the fission mixture.

Table 3. Average Masses of Materials in the Fuel (g/fuel rod).^(a)

Material	UO ₂	U	Cu
Average Mass (g/fuel rod)	6.336	5.555	14.34

(a) Reference 2.

Fuel rod clad and caps were made of stainless steel 0X16H15M3E. Its density is 7.90 g/cm³, and its composition is given in Table 4.

Table 4. Composition of Stainless Steels 0X16H15M3B and 1X18H9T.^(a)

Element	0X16H15M3B (wt. %)	1X18H9T (wt. %)
C	≤ 0.09	≤ 0.12
Si	≤ 0.8	≤ 0.18
Mn	≤ 0.6	≤ 2.0
S	≤ 0.02	≤ 0.02
P	≤ 0.035	≤ 0.035
Cr	15-17	18.0
Ni	14-16	10.0
Mo	2.5-3.0	-
Nb	0.6-0.9	-
Cu	≤ 0.3	-
Fe	balance	balance

(a) State Standard of the USSR 5632-72

Table 5 shows the composition of the B2 bronze fuel rod plug. Its density is 8.30 g/cm³.

Table 5. Composition of the B2 Bronze Fuel Rod Plug.^(a)

Element	Wt.%
Ni	0.2 - 0.5
Be	1.9 - 2.2
Cu	balance

(a) I. K. Kikoin et al., Handbook "The Tables of Physical Quantities," Atomizdat, M. 1976, page 47.

1.3.2 Absorber Rod Material Data - Absorber rod clad was made of stainless steel 0X16H15M3B (see Table 4). Absorber rod bottom steel plugs were made of stainless steel 1X18H9T. Its density is 7.90 g/cm³. Its composition is also given in Table 4.

Two types of absorbers were used in the experiments: a Gd₂O₃ and Al₂O₃ mixture at a density of 1.31 ± 0.05 g/cm³, and a Sm₂O₃ and Al₂O₃ mixture at a density of 1.59 ± 0.05 g/cm³. The uncertainty of the densities of Gd₂O₃ and Sm₂O₃ was not more than 2 %. Tables 6 and 7 show the compositions of the absorbers.

The rubber plugs used in the absorber rods were frozen in liquid nitrogen before they were inserted in the rods. The rubber's measured density is 1.07 g/cm³. Table 8 shows the composition of the rubber plugs.

Table 6. Composition of Gd Absorber.^(a)

Element	Wt.%
Gd	6.21
Al	49.14
O	44.65

(a) Reference 2.

Table 7. Composition of Sm Absorber.^(a)

Element	Wt.%
Sm	34.64
Al	31.67
O	33.69

(a) Reference 2.

Table 8. Composition of the Rubber.^(a)

Element	Wt.%
C	84
H	11
S	5

(a) Reference 2.

1.3.3 Structural Components of the Assembly - Lattice and support plates were made of AD1 aluminium alloy. Its density is 2.71 g/cm³. Its composition is given in Table 9.^a

^a A. G. Samoylov, "The Heating Elements of the Nuclear Reactor Cores," M. Energoatomizdat 1985, page 162.

Table 9. Composition of AD1 Alloy.

Element	Wt. %
Fe	0.3
Si	0.35
Cu	0.05
Al	balance

The fuel rod support plate was made of Plexiglas ($C_5H_8O_2)_n$. Its measured density is 1.18 g/cm³.

1.3.4 Distilled Water - Density of distilled water is 0.9982 g/cm³ at T=20 °C.^a Table 10 shows the impurity contents of the distilled water.

Table 10. Impurities in the Distilled Water.

Material	Wt. %
chlorides	< $5.0 \cdot 10^{-8}$
salts	< $1.0 \cdot 10^{-6}$
solid residuals	< $1.0 \cdot 10^{-7}$

1.4 Supplemental Experimental Measurements

No supplemental experimental measurements were found.

^a CRC Handbook of Chemistry and Physics, 68th edition, page F-10.

2.0 EVALUATION OF EXPERIMENTAL DATA

Experiments were carefully performed and well documented. Most of the data were taken from Reference 2. Some details of the experiments were not published, but were taken from logbooks. There were no significant omissions of data.

The combined uncertainties in k_{eff} are mainly defined by the geometrical and material composition uncertainties. The uncertainty in k_{eff} due to other factors (see Section 1.2.1) is no more than $\sim 4 \cdot 10^{-4}$.

2.1 Fuel Rod and Absorber Rods Data

The main uncertainties in the characterization of the fuel rods are connected with uncertainties of mass of ^{235}U and of geometrical dimensions. The average mass of ^{235}U in the fuel rods used in these experiments could be derived from an analysis of the fuel rod certifications. Their standard deviations (1σ) were 0.035-0.040 %.

The main geometrical uncertainties are connected with uncertainties in fuel length and in cross section of the spiral cross-shaped fuel rods, which was due partially to uncertainties of the rod clad inner and outer diameters. Concerning the latter, after additional consultations with representatives of the fuel rod manufacturing plant, it was concluded that a reasonable estimate for the uncertainty of the cross sectional area of the fuel rod is 2.5%.

The measured fuel length, 341 mm, was chosen as the fuel region height of the benchmark model. Its uncertainty can be evaluated as ± 4 mm (see Section 1.2 and Figure 4).

Another geometrical uncertainty is lattice pitch. The uncertainty in pitch value of the fuel rod lattice can be evaluated as ± 0.002 cm (standard deviation 1σ).

The uncertainty of the absorber mass in the mixture Gd_2O_3 (or Sm_2O_3) with Al_2O_3 of a single rod can be evaluated as $\pm 2\%$ (standard deviation 1σ). Dividing by the square root of the corresponding number of absorber rods used in the experiments gives 0.19% (Case 1), 0.27% (Case 2), 0.18% (Case 3), and 0.27% (Case 4) uncertainty in fuel mass for these four experiments.

The sensitivities of k_{eff} to uncertainties in fuel and absorber rod characterizations were evaluated by the code PARIS^a. The code PARIS performs a generalized scheme of effective homogenization applicable to any hierarchical structure. The transport group calculation combines neutron transfer for all structural levels with in-level homogenization by flux-weighting of elemental macroscopic cross sections. Transport equations are presented in first-event-probabilities form for isotropically entering neutrons. The thermalization and resonance self-shielding are treated, respectively, by the modified Wigner-Wilkins formalism and Wigner escape approximation.

^a A. G. Promohov, "Code PARIS for Neutron-Physical Calculation of Water Moderated Multilevel Cell. User Manual," Report of RRC "Kurchatov Institute" 31/1-1773-92, 1992.

Table 11, 12, 13, and 14 show the sensitivity of k_{eff} to the main uncertainties of fuel and absorber rods characterization as well as the uncertainties of k_{eff} corresponding to the particular parameter uncertainties.

Table 11. Sensitivity of k_{eff} to Uncertainties in Fuel Rod and Gadolinium Rod Characterization for the First Critical Configuration (Case 1). The pitch of gadolinium rods is ~27.5 mm (see Figure 7 and Table 1).

Parameter	% Uncertainty of the Parameter (1σ)	% k_{eff}
Pitch	0.37	0.047
Uranium Mass	0.038	0.007
Gadolinium Mass	0.19	0.003
Fuel Rod Cross Section Area	2.5	0.290
Fuel Length	3.0	0.216
Total uncertainty of $k_{\text{eff}}\text{ (%)}$		0.37

Table 12. Sensitivity of k_{eff} to Uncertainties in Fuel Rod and Gadolinium Rod Characterization for the Second Critical Configuration (Case 2). The pitch of gadolinium rods is ~36.7 mm (see Figure 8 and Table 1).

Parameter	% Uncertainty of the Parameter (1σ)	% k_{eff}
Pitch	0.37	0.051
Uranium Mass	0.040	0.007
Gadolinium Mass	0.27	0.002
Fuel Rod Cross Section Area	2.5	0.308
Fuel Length	3.0	0.210
Total uncertainty of $k_{\text{eff}}\text{ (%)}$		0.38

Table 13. Sensitivity of k_{eff} to Uncertainties in Fuel Rod and Samarium Rod Characterization for the Third Critical Configuration (Case 3). The pitch of samarium rods is ~27.5 mm (see Figure 9 and Table 1).

Parameter	% Uncertainty of the Parameter (1σ)	% k_{eff}
Pitch	0.37	0.051
Uranium Mass	0.035	0.007
Samarium Mass	0.18	0.005
Fuel Rod Cross Section Area	2.5	0.293
Fuel Length	3.0	0.204
Total uncertainty of $k_{\text{eff}}\ (%)$		0.36

Table 14. Sensitivity of k_{eff} to Uncertainties in Fuel Rod and Samarium Rod Characterization for the Fourth Critical Configuration (Case 4). The pitch of samarium rods is ~36.7 mm (see Figure 10 and Table 1).

Parameter	% Uncertainty of the Parameter (1σ)	% k_{eff}
Pitch	0.37	0.053
Uranium Mass	0.038	0.006
Samarium Mass	0.27	0.004
Fuel Rod Cross Section Area	2.5	0.309
Fuel Length	3.0	0.201
Total uncertainty of $k_{\text{eff}}\ (%)$		0.37

The uncertainties in measured parameters are small, and all relevant experimental parameters are known. Therefore all these experiments are acceptable for use as benchmark experiments.

3.0 BENCHMARK SPECIFICATIONS

3.1 Description of Model

The benchmark model follows, in general, the experiment description given in Section 1, with the following exceptions:

1. The real geometry of the spiral cross-shaped fuel rod could not be reproduced by any known computer code. However, the effect of the "spirality", that is to say, the difference in k_{eff} due to the substitution of the spiral cross-shaped fuel rod by the straight one, is determined by the influence of the difference in the mutual orientation of the fuel rods. The quantity of this effect could be estimated by the difference in k_{eff} between two lattices of the straight cross-shaped fuel rods: the fuel rods in one lattice are twisted clockwise by 45 degrees relative to the fuel rods of the other lattice. Such evaluations were performed with MCNP. The difference in k_{eff} due to this effect is smaller than 0.0008 (this quantity is restricted by the statistical uncertainty of the Monte-Carlo method).

To estimate the possibility of modeling cross-shaped fuel rods by cylindrical rods, calculations of k_{eff} were carried out for the lattice pitch value 0.53 cm for both models of the fuel rods. The difference in k_{eff} due to replacing straight cross-shaped fuel rods by cylindrical fuel rods having the same volumes of fuel and cladding, is smaller than 0.0006. Therefore, the cylindrical model of the spiral cross-shaped fuel rods was used in models of these experiments.

2. Since measurements of the effects of removal of the tubes containing neutron detectors and the tubes of the control and safety rods indicated that they had no significant influence on critical conditions, these tubes were excluded from the model.
3. The two lattice plates were omitted from the model based on engineering judgment.
4. The stand of aluminum alloy (see Figures 1 and 2) was also excluded from the model because of its negligible influence on critical conditions.
5. The tapered ends of the bronze plugs and absorber rod end caps can be replaced by straight ends with negligible effect.

3.2 Dimensions

Fuel rod dimensions, as modeled, are shown in Figure 11. The cladding outer radius is 1.7598 mm, the fuel and bronze plug radii are 1.5165 mm, and the radius of the end caps is 1 mm.

Absorber rod dimensions are shown in Figure 6. (The tapered plug end is replaced by a cylindrical one of diameter 5.1 mm.) The bottoms of the absorber rods are 8 mm above the bottoms of the fuel rods (see Figure 3).

The model of the bottom reflector corresponds to Figure 1 and Figure 3 and consists of five layers:

- 1- 25 mm Plexiglas support plate;
- 2- 15 mm aluminum alloy AD1 support plate;
- 3- 100 mm layer of water.
- 4- 20 mm aluminum alloy AD1 support plate;
- 5- 200 mm layer of water.

The top and side reflectors are modelled by 300 mm water layers.

Lattice configurations are shown in Figures 7 - 10.

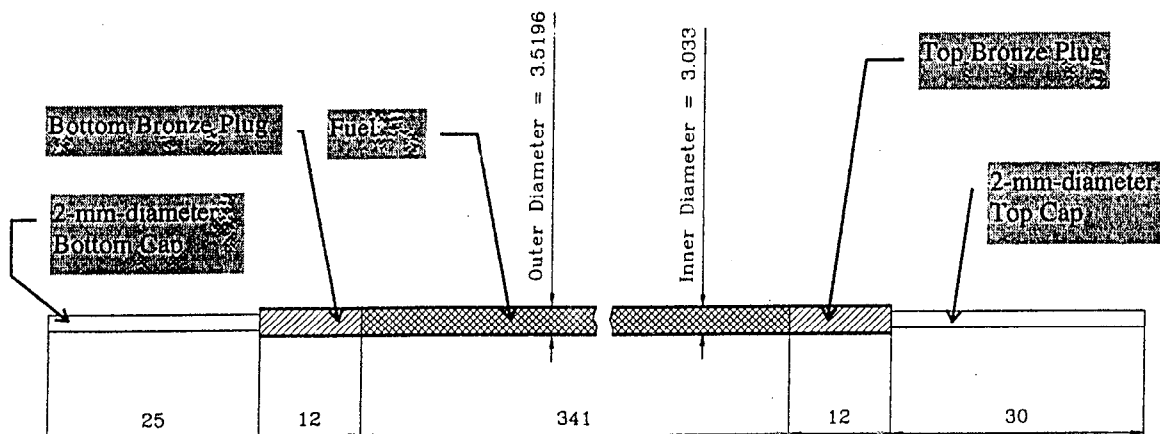


Figure 11. Cylindrical Model of the Fuel Rod. (dimensions given in mm)

3.3 Material Data

Nine materials were identified for the four experiments. They are summarized in Table 15.

Table 15. Summary of Experimental Model Materials.

Material Number	Material Description	Density (g/cm ³)	Element	Wt.%	Atom Density (atoms/barn·cm)
1	Water (H ₂ O) ^(a)	0.9982	H O	11.19 88.81	6.6736x10 ⁻² 3.3368x10 ⁻²
2	Aluminum alloy AD1	2.71	Al Si Fe Cu	99.3 0.35 0.3 0.05	6.0062x10 ⁻² 2.0337x10 ⁻⁴ 8.7667x10 ⁻⁵ 1.2841x10 ⁻⁵
3	Stainless steel 0X16H15M3B (Fuel rod cladding and end caps and absorber rod cladding)	7.90	C Si Cr Fe Ni Nb Mo	0.09 0.8 16.0 64.21 15.0 0.9 3.0	3.5648x10 ⁻⁴ 1.3551x10 ⁻³ 1.4639x10 ⁻² 5.4698x10 ⁻² 1.2159x10 ⁻² 4.6086x10 ⁻⁴ 1.4876x10 ⁻³
4	Plexiglas	1.18	H O C	8.06 31.96 59.98	5.6826x10 ⁻² 1.4194x10 ⁻² 3.5486x10 ⁻²
5	Fuel	8.3922	²³⁴ U ²³⁵ U ²³⁶ U ²³⁸ U O Cu	0.227109 23.84669 0.075453 2.71765 3.777326 69.35577	4.9042x10 ⁻⁵ 5.1275x10 ⁻³ 1.6155x10 ⁻⁵ 5.7696x10 ⁻⁴ 1.1932x10 ⁻² 5.5159x10 ⁻²
6	Bronze	8.30	Ni Be Cu	0.5 2.2 97.3	4.2582x10 ⁻⁴ 1.2201x10 ⁻² 7.6533x10 ⁻²
7	Absorber (Case 1 and Case 2)	1.31	¹⁵² Gd ¹⁵⁴ Gd ¹⁵⁵ Gd ¹⁵⁶ Gd ¹⁵⁷ Gd ¹⁵⁸ Gd ¹⁶⁰ Gd Al O	0.011999 0.13251 0.905465 1.260435 0.969837 1.549156 1.380598 49.14 44.65	6.2309x10 ⁻⁷ 6.7917x10 ⁻⁶ 4.6109x10 ⁻⁵ 6.3773x10 ⁻⁵ 4.8757x10 ⁻⁵ 7.7388x10 ⁻⁵ 6.8104x10 ⁻⁵ 1.4368x10 ⁻² 2.2016x10 ⁻²
7	Absorber (Case 3 and Case 4)	1.59	Sm Al O	34.64 31.67 33.690	2.2059x10 ⁻³ 1.1239x10 ⁻² 2.0162x10 ⁻²
8	Stainless steel 1X18H9T (Plug of absorber rod)	7.90	C Si Mn Cr Fe	0.12 0.18 2.0 18.0 69.7	4.7531x10 ⁻⁴ 3.0490x10 ⁻⁴ 1.7319x10 ⁻³ 1.6469x10 ⁻² 5.9375x10 ⁻²

Material Number	Material Description	Density (g/cm ³)	Element	Wt.%	Atom Density (atoms/barn·cm)
			Ni	10.0	8.1060x10 ⁻³
9	Rubber	1.07	C	84.0	4.5064x10 ⁻²
			H	11.0	7.0324x10 ⁻²
			S	5.0	1.0047x10 ⁻³

(a) Because their effect is judged to be negligible, water impurities are not included (see Table 10).

3.4 Temperature Data

The temperature of the critical assemblies varied in the range from 18°C to 20°C. In the model T=300 K was used for all zones of the assemblies.

3.5 Experimental and Benchmark-Model k_{eff}

The experimental k_{eff} 's were 1.000.

The uncertainties in k_{eff} were discussed in Section 2. Including the 0.0006 uncertainty from using a cylindrical rather than a cross-shaped model, benchmark-model k_{eff} 's are:

for Case 1 $k_{eff}=1.0000 \pm 0.0038$

for Case 2 $k_{eff}=1.0000 \pm 0.0039$

for Case 3 $k_{eff}=1.0000 \pm 0.0037$

for Case 4 $k_{eff}=1.0000 \pm 0.0038$.

4.0 RESULTS OF SAMPLE CALCULATIONS

Results of calculations are presented in Table 16. They give the $k_{\text{eff}} \pm 1\sigma$ results for MCNP using continuous-energy ENDF/B-V cross section. Input listings are presented in Appendix A.

Table 16. Results of Sample Calculations (United States).^(a)

Code (Cross Section Set) → Case Number ↓	MCNP (Continuous-Energy ENDF/B-V)
1	0.9926 ± 0.0015
2	0.9904 ± 0.0012
3	0.9988 ± 0.0012
4	0.9955 ± 0.0012

(a) Results supplied by the authors.

5.0 REFERENCES

1. A. Yu. Gagarinski, E. S. Glushkov, N. N. Ponomarev-Stepnoi, "A Short Review of Critical Experiments with Highly , Intermediate and Low Enriched Uranium Systems Performed at Kurchatov Institute," Presentation of Nuclear Critical Technology Safety Meeting, Williamsburg, Virginia , USA, May 10 and 11, 1994.
2. A. Yu. Gagarinski et al., "Critical Experiments with Water Moderated Heterogeneous Lattices of Highly Enriched Fuel Rods," Preprint IAE 5934/4, 1995.

APPENDIX A: TYPICAL INPUT LISTINGS

A.1 MCNP Input Listings

The MCNP4a calculations used 500 generations at 1000 neutrons per generation. Ten generations were skipped before averaging, resulting in 490,000 neutron histories.

HEU-COMP-THERM-004

MCNP Input Listing: Case 1, Table 16.

4 PZ 20.0 \$ bottom plane of 20-mm-support plate
 5 PZ 22.0 \$ top plane of 20-mm-support plate
 6 PZ 32.0 \$ bottom plane of 15-mm-support plate
 7 PZ 33.5 \$ top plane of 15-mm-support plate
 8 PZ 36.0 \$ bottom of the fuel rod
 9 PZ 36.8 \$ bottom of the absorber rod
 10 PZ 38.5 \$ top plane of bottom cap
 11 PZ 39.7 \$ bottom plane of fuel/absorber region
 12 PZ 38.25 \$ bottom plane of rubber plug
 13 PZ 73.8 \$ top plane of fuel region
 14 pz 74.7 \$ top plane of absorber region
 15 pz 77.3 \$ top edge of absorber rod
 16 pz 75 \$ bottom plane of top cap
 17 pz 78 \$ top edge of fuel rod
 18 CZ 15.4 \$ radius of the core
 19 CZ 0.1 \$ fuel cap radius
 20 CZ 0.15165 \$ fuel radius
 21 CZ 0.17598 \$ fuel rod clad radius
 22 cz 0.225 \$ absorber radius
 23 cz 0.255 \$ absorber rod clad radius
 c reflecting surfaces
 *101 PY 0.0
 *102 P -0.8660254 0.5 0.0 0.0
 C elementary cell surfaces
 201 PX 0.265
 202 PX -0.265
 203 P 0.305996 0.53 0.0 0.162178
 204 P 0.305996 0.53 0.0 -0.162178
 205 P -0.305996 0.53 0.0 0.162178
 206 P -0.305996 0.53 0.0 -0.162178
 IMP:N 0 1 21R
 KSRC -0.53 0.05 56.75
 KCODE 1000 1.0 10 500
 m1 lwrt.01
 c water n= 0.100104 (0.9982 g/cm3)
 m1 1001.50c 6.6736e-2
 8016.50c 3.3368e-2
 C aluminum alloy AD1 n= 0.06036588 (2.71 g/cm3)
 M2 13027.50c 6.0062e-2
 14000.50c 2.0337e-4
 26000.50c 8.7667e-5
 29000.50c 1.2841e-5
 c cladding of stainless steel n= 0.08515604 (7.9 g/cm3)
 m3 6000.50c 3.5648e-4
 14000.50c 1.3551e-3
 24000.50c 1.4639e-2
 26000.50c 5.4698e-2
 28000.50c 1.2159e-2
 41093.50c 4.6086e-4
 42000.50c 1.4876e-3
 C Plexiglas n= 0.106506 (1.18 g/cm3)
 m4 1001.50c 5.6826e-2
 8016.50c 1.4194e-2
 6012.50c 3.5486e-2
 c fuel n= 0.072860657 (8.3922 g/cm3)
 m5 92234.50c 4.9042e-5
 92235.50c 5.1275e-3
 92236.50c 1.6155e-5

1 PZ 0.0 \$ bottom plane of the model
 2 PZ 98.0 \$ top plane of the model
 3 CZ 45.4 \$ external radius of the model

NEA/NSC/DOC/(95)03/II
Volume II

HEU-COMP-THERM-004

MCNP Input Listing: Case 1, Table 16 (cont'd).

```
92238.50c 5.7696e-4
8016.50c 1.1932e-2
29000.50c 5.5159e-2
c bronze B2 n= 0.08915982 (8.30 g/cm3)
m6 28000.50c 4.2582e-4
4009.50c 1.2201e-2
29000.50c 7.6533e-2
c Gd absorber n= 0.036695546 (1.31 g/cm3)
m7 64152.50c 6.2309e-7
64154.50c 6.7917e-6
64155.50c 4.6109e-5
64156.50c 6.3773e-5
64157.50c 4.8757e-5
64158.50c 7.7388e-5
64160.50c 6.8104e-5
13027.50c 1.4368e-2
8016.50c 2.2016e-2
c plug of absorber rod n= 0.08646211 (7.9 g/cm3)
m8 6000.50c 4.7531e-4
14000.50c 3.0490e-4
25055.50c 1.7319e-3
24000.50c 1.6469e-2
26000.50c 5.9375e-2
28000.50c 8.1060e-3
c rubber n= 0.1163927 1.07 g/cm3
m9 6000.50c 4.5064e-2
1001.50c 7.0324e-2
16032.50c 1.0047e-3
```

HEU-COMP-THERM-004

MCNP Input Listing: Case 2, Table 16.

MCNP Input Listing: Case 2, Table 16 (cont'd).

```
4009.50c 1.2201e-2
29000.50c 7.6533e-2
c Gd absorber n= 0.036695546 (1.31 g/cm3)
m7 64152.50c 6.2309e-7
    64154.50c 6.7917e-6
    64155.50c 4.6109e-5
    64156.50c 6.3773e-5
    64157.50c 4.8757e-5
    64158.50c 7.7388e-5
    64160.50c 6.8104e-5
    13027.50c 1.4368e-2
    8016.50c 2.2016e-2
c plug of absorber rod n= 0.08646211 (7.9 g/cm3)
m8 6000.50c 4.7531e-4
    14000.50c 3.0490e-4
    25055.50c 1.7319e-3
    24000.50c 1.6469e-2
    26000.50c 5.9375e-2
    28000.50c 8.1060e-3
c rubber n= 0.1163927 1.07 g/cm3
m9 6000.50c 4.5064e-2
    1001.50c 7.0324e-2
    16032.50c 1.0047e-3
```

HEU-COMP-THERM-004

MCNP Input Listing: Case 3, Table 16.

NEA/NSC/DOC/(95)03/II
Volume II

HEU-COMP-THERM-004

MCNP Input Listing: Case 3, Table 16 (cont'd).

```
29000.50c 5.5159e-2
c  bronze B2 n= 0.08915982 (8.30 g/cm3)
m6 28000.50c 4.2582e-4
  4009.50c 1.2201e-2
  29000.50c 7.6533e-2
c  Sm absorber n= 0.0336069 (1.59 g/cm3)
m7 62000.00c 2.2059e-3
  13027.50c 1.1239e-2
  8016.50c 2.0162e-2
c  plug of absorber rod n= 0.08646211 (7.9 g/cm3)
m8 6000.50c 4.7531e-4
  14000.50c 3.0490e-4
  25055.50c 1.7319e-3
  24000.50c 1.6469e-2
  26000.50c 5.9375e-2
  28000.50c 8.1060e-3
c  rubber n= 0.1163927 1.07 g/cm3
m9 6000.50c 4.5064e-2
  1001.50c 7.0324e-2
  16032.50c 1.0047e-3
```

HEU-COMP-THERM-004

MCNP Input Listing: Case 4, Table 16.

1 PZ 0.0 \$ bottom plane of the model
 2 PZ 98.0 \$ top plane of the model
 3 CZ 45.4 \$ external radius of the model
 4 PZ 20.0 \$ bottom plane of 20-mm-support plate

5 PZ 22.0 \$ top plane of 20-mm-support plate
 6 PZ 32.0 \$ bottom plane of 15-mm-support plate
 7 PZ 33.5 \$ top plane of 15-mm-support plate
 8 PZ 36.0 \$ bottom of the fuel rod
 9 PZ 36.8 \$ bottom of the absorber rod
 10 PZ 38.5 \$ top plane of bottom cap
 11 PZ 39.7 \$ bottom plane of fuel/absorber region
 12 PZ 38.25 \$ bottom plane of rubber plug
 13 PZ 73.8 \$ top plane of fuel region
 14 pz 74.7 \$ top plane of absorber region
 15 pz 77.3 \$ top edge of absorber rod
 16 pz 75 \$ bottom plane of top cap
 17 pz 78 \$ top edge of fuel rod
 18 CZ 15.4 \$ radius of the core
 19 CZ 0.1 \$ fuel cap radius
 20 CZ 0.15165 \$ fuel radius
 21 CZ 0.17598 \$ fuel rod clad radius
 22 cz 0.225 \$ absorber radius
 23 cz 0.255 \$ absorber rod clad radius
 c reflecting surfaces
 *101 PY 0.0
 *102 P -0.8660254 0.5 0.0 0.0
 C elementary cell surfaces
 201 PX 0.265
 202 PX -0.265
 203 P 0.305996 0.53 0.0 0.162178
 204 P 0.305996 0.53 0.0 -0.162178
 205 P -0.305996 0.53 0.0 0.162178
 206 P -0.305996 0.53 0.0 -0.162178

 IMP:N 0 1 21R
 KSRC -0.53 0.05 56.75
 KCODE 1000 1.0 10 500
 mt1 lwrtr.01
 c water n= 0.100104 (0.9982 g/cm3)
 m1 1001.50c 6.6736e-2
 8016.50c 3.3368e-2
 C aluminum alloy AD1 n= 0.06036588 (2.71 g/cm3)
 M2 13027.50c 6.0062e-2
 14000.50c 2.0337e-4
 26000.50c 8.7667e-5
 29000.50c 1.2841e-5
 c cladding of stainless steel n= 0.08515604 (7.9 g/cm3)
 m3 6000.50c 3.5648e-4
 14000.50c 1.3551e-3
 24000.50c 1.4639e-2
 26000.50c 5.4698e-2
 28000.50c 1.2159e-2
 41093.50c 4.6086e-4
 42000.50c 1.4876e-3
 C Plexiglas n= 0.106506 (1.18 g/cm3)
 m4 1001.50c 5.6826e-2
 8016.50c 1.4194e-2
 6012.50c 3.5486e-2
 c fuel n= 0.072860657 (8.3922 g/cm3)
 m5 92234.50c 4.9042e-5
 92235.50c 5.1275e-3
 92236.50c 1.6155e-5
 92238.50c 5.7696e-4
 8016.50c 1.1932e-2
 29000.50c 5.5159e-2
 c bronze B2 n= 0.08915982 (8.30 g/cm3)
 m6 28000.50c 4.2582e-4
 4009.50c 1.2201e-2
 29000.50c 7.6533e-2
 c Sm absorber n= 0.0336069 (1.59 g/cm3)
 m7 62000.00c 2.2059e-3
 13027.50c 1.1239e-2
 8016.50c 2.0162e-2

NEA/NSC/DOC/(95)03/II
Volume II

HEU-COMP-THERM-004

MCNP Input Listing: Case 4, Table 16 (cont'd).

c plug of absorber rod n= 0.08646211 (7.9 g/cm³)

m8 6000.50c 4.7531e-4

14000.50c 3.0490e-4

25055.50c 1.7319e-3

24000.50c 1.6469e-2

26000.50c 5.9375e-2

28000.50c 8.1060e-3

c rubber n= 0.1163927 1.07 g/cm³

m9 6000.50c 4.5064e-2

1001.50c 7.0324e-2

16032.50c 1.0047e-3